Contribution from the Department of Chemistry,
City University of New York, Queens College, Flushing, New York 11367

# Photochemistry of Group 6B Hexacarbonyls Adsorbed onto Porous Vycor Glass. Evidence for the Formation of Methane from Carbon Species in the Glass

Robert C. Simon, Edgar A. Mendoza, and Harry D. Gafney*

*Received October 8, 1987*

$Cr(CO)_6$, $Mo(CO)_6$, and $W(CO)_6$ physisorb onto porous Vycor glass without disruption of the primary coordination spheres. UV photolysis of the adsorbed complexes leads to decarbonylation and formation of the corresponding pentacarbonyl, where the vacated coordination site is most likely occupied by a silanol oxygen. With 350-nm excitation, the quantum yields for decarbonylation of $Mo(CO)_6$ and $W(CO)_6$ are similar to those found in fluid solution, whereas that for $Cr(CO)_6$ is significantly reduced. Continued photolysis with 350-nm light causes further decarbonylation, whereas 310- and 254-nm photolysis leads to CO, $CH_4$, $H_2$, and $CO_2$ evolution. $CH_4$ evolution initiates when the complex achieves an average molecularity of $M(CO)_4$ and initially occurs in a 1:1 stoichiometric ratio with a concurrent oxidation of the mononuclear complex. The metal oxide agglomerates on the glass surface, and excitation of the agglomerate continues $CH_4$ evolution. Diffuse-reflectance FTIR spectra reveal formaldehyde and methanol intermediates. However, GC analysis and $^{13}C$-labeling experiments establish that $CH_4$ does *not* derive from the initially coordinated CO. Rather, $CH_4$ evolution is attributed to a metal-promoted hydrogenation of a $C_1$ oxide within the glass matrix.

## Introduction

Interest in the photoactivation of transition-metal carbonyls stems in part from their potential use as photocatalysts.[1] Wrighton and others, for example, have demonstrated the catalytic activity of products derived from the photolyses of $M(CO)_6$ (M = Cr, Mo, and W) complexes.[2-5] Although the majority of work has focused on photocatalytic behavior in homogeneous solution, recent studies have begun to explore the photoactivation of surface-confined metal carbonyls[6-13] as an alternate route to hybrid catalysts.[14] Implicit in this approach, however, is an understanding of the photochemical behavior of a surface-confined metal carbonyl.

Unless adsorption onto the support changes the complex, the primary photochemical event of a physisorbed metal carbonyl is equivalent to that in fluid solution.[10-13] On the other hand, the products derived from the reaction can be quite different from those obtained in fluid solution. Jackson and Thrushiem, for example, find that photolysis of $Fe(CO)_5$ physisorbed onto silica gel yields $Fe_3(CO)_{12}$[10] whereas photolysis in the gas or liquid phases and in noncoordinating solvents yields $Fe_2(CO)_9$.[15-18] In contrast to the substitution and fragmentation reactions in homogeneous solution,[20] photolysis of $Ru_3(CO)_{12}$ physisorbed onto porous Vycor glass leads to quantitative formation of the oxidative-addition product $(\mu\text{-H})Ru_3(CO)_{10}(\mu\text{-OSi})$.[13] These changes in reactivity arise in the secondary thermal and/or photochemical reactions. Unlike a noncoordinating solvent, a hydroxylated support, in particular, can function as a polydentate ligand, where binding to a surface functionality can stabilize a photoproduct, influence its spectral properties, and curtail its mobility.[10,11,19] In addition, although less well understood at present, the dimensionality, i.e., the irregularity of the surface, may be a further constraint on adsorbate reactivity.[21] Each or any combination of these parameters will influence the reactivity of a surface-confined complex.

To circumvent the difficulties imposed by the opacity of more traditional supports,[10] we have examined the photochemical behavior of the group 6B hexacarbonyls on porous Vycor glass (PVG) and, in this paper, describe the results of these experiments. The similarities between PVG, a transparent, surface-hydroxylated silica with a myriad of randomly dispersed 70 ± 21 Å diameter pores, and silica gel have been described.[22-24] Irradiation of $M(CO)_6$(ads) (ads denotes the adsorbed complex) with 350-nm light causes a progressive decarbonylation of the complex, whereas irradiation with 310- or 254-nm light leads to the concurrent evolution of $CH_4$, $H_2$, and trace amounts of $CO_2$. However, GC analyses and $^{13}C$-labeling experiments establish that $CH_4$ does *not* derive from the coordinated CO. Rather, photoactivation of the complex promotes the hydrogenation of a $C_1$ oxide within the glass matrix.

## Experimental Section

**Materials.** $Cr(CO)_6$, $Mo(CO)_6$, and $W(CO)_6$ (Pressure Chemical Co.) were used without further purification since their UV–visible and infrared spectra were in excellent agreement with published spectra.[25,26] $W(^{13}CO)_6$ (Pressure Chemical Co.) was also used without further purification since its UV–visible spectrum also agreed with published spectra.[25] The claimed enrichment (90%) was confirmed by mass spectroscopy and the integrated relative intensities (8.8:1) of the 1844- and 1986-$cm^{-1}$ $^{13}CO$ and CO bands. $[(C_2H_5)_4N][HW(CO)_5]$ was prepared under nitrogen according to the method of Gibson and co-workers,[27] and after several washings with hexane, the IR spectrum of the yellow-orange powder agreed with the reported spectrum.[27] $WO_3$ (Pfaltz and Bauer, 99.75%) and $D_2O$ (Norell, 99%) were used as received. Gaseous reagents (Linde) were used without further purification since each had a purity

(1) Wrighton, M. S. *Ann. N.Y. Acad. Sci.* **1980**, *333*, 188–207.
(2) Wrighton, M. S.; Ginley, D. S.; Schroeder, M. A.; Morse, D. L. *Pure Appl. Chem.* **1975**, *41*, 671–679.
(3) Wrighton, M. S.; Schroeder, M. A. *J. Am. Chem. Soc.* **1973**, *95*, 5764–5765.
(4) Wrighton, M. S. *Inorg. Chem.* **1974**, *13*, 905–909.
(5) Nasielski, J.; Kirsch, P.; Wilputte-Steinert, L. *J. Organomet. Chem.* **1971**, *27*, C13–14.
(6) Kinney, J. B.; Staley, R. H.; Reichel, C. L.; Wrighton, M. S. *J. Am. Chem. Soc.* **1981**, *103*, 4273–4275.
(7) Reichel, C. L.; Wrighton, M. S. *J. Am. Chem. Soc.* **1981**, *103*, 7180–7189; *Inorg. Chem.* **1980**, *19*, 3858–3863.
(8) Liu, D. K.; Wrighton, M. S. *J. Am. Chem. Soc.* **1982**, *104*, 898–902.
(9) Klein, B.; Kazlauskas, R. J.; Wrighton, M. S. *Organometallics* **1982**, *1*, 1338–1350.
(10) Jackson, R. L.; Thrusheim, M. R. *J. Am. Chem. Soc.* **1982**, *104*, 6590–6596.
(11) Simon, R. C.; Gafney, H. D.; Morse, R. L. *Inorg. Chem.* **1983**, *22*, 573–574.
(12) Darsillo, M. S.; Gafney, H. D.; Paquette, M. S. *J. Am. Chem. Soc.* **1987**, *109*, 3275–3286.
(13) Dieter, T.; Gafney, H. D. *Inorg. Chem.* **1988**, *27*, 1730–1736.
(14) Bailey, D. C.; Langer, S. H. *Chem. Rev.* **1981**, *81*, 109–148.
(15) Graham, W. A. G.; Jetz, W. *Inorg. Chem.* **1971**, *10*, 4–9.
(16) Chisholm, M. H.; Massey, A. G.; Thompson, N. R. *Nature (London)* **1966**, *211*, 67.
(17) Dewar, J.; Jones, H. O. *Proc. R. Soc. London, Ser. A* **1905**, *76*, 558–577.
(18) Braye, E. H.; Huebel, W. *Inorg. Synth.* **1966**, *8*, 178–181.
(19) Jackson, R. L.; Thrusheim, M. R. *J. Phys. Chem.* **1983**, *87*, 1910–1916.
(20) Desrosiers, M. F.; Wink, D. A.; Trautman, R.; Friedman, A. E.; Ford, P. C. *J. Am. Chem. Soc.* **1986**, *108*, 1917–1927.
(21) Pfeifer, P.; Avnir, D. *J. Chem. Phys.* **1983**, *79*, 3558–3565.
(22) Iler, R. K. *The Chemistry of Silica*; Wiley-Interscience: New York, 1979; p 551.
(23) Hair, M. L.; Chapman, I. D. *J. Am. Ceram. Soc.* **1966**, *49*, 651–660; *Trans. Faraday Soc.* **1965**, *61*, 1507–1510.
(24) Cant, N. W.; Little, L. H. *Can. J. Chem.* **1964**, *42*, 802–809; **1965**, *43*, 1252–1254.
(25) Wrighton, M. *Chem. Rev.* **1974**, *74*, 401–430.
(26) Magee, T. A.; Matthews, C. N.; Wang, T. S.; Wotiz, J. H. *J. Am. Chem. Soc.* **1961**, *83*, 3200–3203.
(27) Gibson, D. H.; Ahmed, F. U. *Organometallics* **1982**, *1*, 679–681.

0020-1669/88/1327-2733$01.50/0 

level of ≥99%. All solvents were HPLC grade (Fisher Scientific) and were dried over molecular sieves prior to use.

Code 7930 porous Vycor glass containing 70 ± 21 Å cavities was obtained from the Corning Glass Co. and used either as a fine powder (320 or 60–80 mesh) or as 25 mm × 25 mm × 4 mm plates. The glass samples were continuously extracted, first with acetone for 12 h and then with distilled water for an equivalent time. The extracted samples were dried under reduced pressure and then calcined either in air or under flowing $O_2$ or $H_2$ at 650 °C for ≥72 h. The calcined samples were transferred while hot, ca. 500 °C, either directly to a photolysis cell or to a vacuum desiccator and cooled to room temperature under vacuum ($p \leq 10^{-4}$ Torr).

Deuteriation was accomplished by refluxing either powdered or plate samples of the calcined glass in $D_2O$ (Norell, 99%). After they were refluxed for 8–12 h, the samples were dried under vacuum ($p \leq 10^{-4}$ Torr) at room temperature. Integration of the intensities of the 3744- and 2760-$cm^{-1}$ bands of the silanol group and its deuteriated analogue indicated that 33–50% of the Si–OH groups had been converted to Si–OD.

**Impregnation.** Impregnation was by conventional procedures in which calcined samples were exposed to 50 mL of a *n*-hexane solution $10^{-6}$–$10^{-3}$ M in the hexacarbonyl. The moles of complex adsorbed, which ranged from $10^{-7}$ to $10^{-4}$ mol/g of PVG for the 25 mm × 25 mm × 4 mm pieces and as high as $10^{-3}$ mol/g of PVG for the glass powder, was calculated from the change in optical density of the solution phase.[28,29] Hexane incorporated during impregnation was removed under vacuum ($p \leq 10^{-4}$ Torr) at room temperature. Removal of the solvent is a crucial point, and the drying procedure was examined by diffuse-reflectance FTIR (DRIFT) and mass spectral measurements. DRIFT spectra recorded as a function of time showed that the C–H bands of *n*-hexane disappeared from the powdered glass after ca. 20 min of pumping ($p \leq 10^{-3}$ Torr) at room temperature. In the mass spectral measurements, a cell containing a freshly impregnated 25 mm × 25 mm × 4 mm sample was attached to a vacuum line and pumped on. After various pumping times, the cell was closed off, and after equilibration, the mass spectrum of the vapor phase was recorded. No peaks indicative of *n*-hexane fragmentation or fragmentation of other hydrocarbons were detected for samples that had been pumped on for ≥30 min. Consequently, all samples impregnated by these solution procedures were pumped on for ≥30 min, and in some cases as long as 8 h, to ensure solvent removal.

In the absence of a solvent, impregnation was by sublimation.[12] A weighed, calcined PVG sample was mounted upright in a rectangular Pyrex cell and attached to a vacuum line. A 25-mL flask containing the solid complex was attached to the line and the entire system evacuated. A water bath (70 °C) was placed around the flask, and the compound was allowed to equilibrate with the adjoining PVG sample. After it was equilibrated for various times, the flask was closed off and the cell and line were reevacuated. The cell was then closed off, and the moles adsorbed onto the PVG was determined by spectral comparison with samples impregnated by the solution procedures.

**Photochemical Procedures.** Impregnated pieces of PVG were rigidly mounted with a Teflon holder in previously described rectangular quartz or Pyrex cells.[28,29] The cell and enclosed sample were evacuated on a line equipped with an oil diffusion pump isolated from the line by a trap at 77 K. Unless otherwise specified, all samples were irradiated under vacuum ($p \leq 10^{-4}$ Torr) in a Rayonet reactor (Southern New England Ultraviolet Corp.) equipped with 254-, 310-, or 350-nm bulbs. The photon flux, typically (2–4) × $10^{-9}$ einstein/($cm^2$ s), was measured with a ferrioxalate solution in a rectangular cell of the same dimensions.[30] Quantum yield measurements were limited to 350-nm excitation since competitive absorption by the glass (50% transmittance (T) at 295 nm vs air) is negligible at this wavelength. UV–visible spectra were recorded during photolysis, and the initial rates of product formation or reactant consumption were calculated according to previously described procedures.[29] Scattering from the glass surface as well as uncertainties in the optical pathlength within the glass, however, introduce an estimated uncertainty of 25% in reported quantum yields.

Gaseous photoproducts were collected and analyzed by previously described GC procedures.[12,13] The GC analyses were calibrated by the addition of known pressures of each gas to the photolysis cell. Collection and transfer of the gas was accomplished with a Toepler pump, and the detector response was linear in the moles of gas in the cell. In the isotopic labeling experiments, the gaseous photoproducts were either collected in the same manner or transferred directly to a mass spectrometer.

**Physical Measurements.** UV–visible spectra were recorded on a Cary 14 or a Tectron 635 spectrophotometer adapted to accommodate the rectangular cells. Adsorbate emission spectra were recorded on a previously described Perkin-Elmer Hitachi MPF-2A emission spectrophotometer.[28,29,31] Infrared spectra of solutions or KBr pellets were recorded on a Perkin-Elmer Model 1330 spectrometer calibrated with polystyrene. DRIFT spectra of crushed (320 mesh) impregnated PVG samples, diluted 30:1 with KBr, were recorded on a Nicolet 20/5DX FTIR instrument equipped with an intensified IR source, an MCTB detector maintained at 77 K, and a Harricks diffuse-reflectance accessory. The interferograms were terminated under Happ–Ganzel apodization and converted to Kubelka–Munk spectra for quantitative comparison. All spectra were ratioed against a background spectrum of blank, calcined PVG diluted 30:1 with KBr. Room- and low-temperature (77 K) EPR spectra were recorded on a IBM-Bruker 200E-SCR spectrometer. Mass spectra were recorded on a Varian MAT CH7 spectrometer calibrated with perfluorokerosene or, in the low-molecular-weight region, with known samples of $CH_4$ or $CO_2$. Solid samples of $W(^{13}CO)_6$ were sublimed into the spectrometer. Gaseous photoproducts were either bled directly from the photolysis cell into the spectrometer or collected in a sample loop that was then vented into the spectrometer. Both procedures gave identical results.

## Results

**Porous Vycor Glass.** DRIFT spectra of PVG recorded as a function of temperature show that the three weight losses during thermal gravimetric analysis[29] correspond to the loss of bulk water (100–120 °C) and chemisorbed water (≥120 °C) up to the onset of consolidation (ca. 700 °C). At the calcination temperature, 650 °C, spectra[13] exhibit a sharp, intense band at 3744 $cm^{-1}$ with a shoulder at 3655 $cm^{-1}$ that have been assigned to free and hydrogen-bonded silanol groups, respectively.[23,24] Spectra of many of the calcined samples also show a weak, broad band at 3500 $cm^{-1}$ that indicates the presence of chemisorbed water. The intensity of this band varies from sample to sample, but in all cases, its intensity after calcination was ≤10% of that of the 3744-$cm^{-1}$ silanol band. Deuteriated PVG exhibits an additional band at 2760 $cm^{-1}$ with a shoulder at 2641 $cm^{-1}$ that are assigned to the deuteriated analogues of the free and associated silanols, respectively.[13] A weak shoulder at higher wavenumbers, which is attributed to the asymmetric stretch of $D_2O$, again indicates the presence of small amounts of chemisorbed $D_2O$ in these samples.

**Adsorption of $Cr(CO)_6$, $Mo(CO)_6$, and $W(CO)_6$.** Electronic spectra of the adsorbed complexes recorded at different locations on a 25 mm × 25 mm × 4 mm sample are identical within experimental error. The spectral agreement establishes that impregnation by either solution adsorption or sublimation leads to a uniform distribution of the hexacarbonyls on the PVG surface.[28,29,31] Regardless of the moles adsorbed, however, each carbonyl complex penetrates no more than 0.5 ± 0.1 mm and impregnates regions adjacent to the outer geometric surfaces of the glass.[11,28,29] A linear decline in adsorbate optical density with thickness, i.e., optical path length, within the impregnated volumes implies a uniform distribution of the complexes within these volumes.[28] Taking the area occupied by $M(CO)_6$(ads) (M = Cr, Mo, W) to be 38.5 $Å^2$ [32] and the surface area to be 130 $m^2/g$,[29] the samples prepared in these experiments, which ranged from $10^{-7}$ to $10^{-3}$ mol/g of PVG, correspond to fractional surface coverages within the impregnated regions of ≤0.0008 to essentially monolayer coverage. Since the complex is not uniformly distributed throughout the entire sample, however, the calculated values are approximations and are used in a relative rather than absolute sense.

**Spectral Properties of $Cr(CO)_6$(ads), $Mo(CO)_6$(ads), and $W(CO)_6$(ads).** The electronic spectra of the adsorbed complexes closely resemble spectra of the complexes in *n*-hexane.[11,25,33] In the 500–260-nm region, spectra of $Cr(CO)_6$(ads), $Mo(CO)_6$(ads), and $W(CO)_6$(ads) show intense bands centered at 280, 286, and 287 nm, respectively. The lower energy, ligand field transitions,

(28) Wolfgang, S.; Gafney, H. D. *J. Phys. Chem.* **1983**, *87*, 5395–5401.
(29) Kennelly, T.; Gafney, H. D.; Braun, M. *J. Am. Chem. Soc.* **1985**, *107*, 4431–4440.
(30) Calvert, J. G.; Pitts, J. N. *Photochemistry*; Wiley: New York, 1971; pp 780–788.
(31) Basu, A.; Gafney, H. D.; Perettie, D. J.; Clark, J. B. *J. Phys. Chem.* **1983**, *87*, 4532–4538.
(32) Beach, N. A.; Gray, H. B. *J. Am. Chem. Soc.* **1968**, *90*, 5713–5721.
(33) Geoffroy, G. L.; Wrighton, M. S. *Organometallic Photochemistry*; Academic: New York, 1979; pp 46–49.

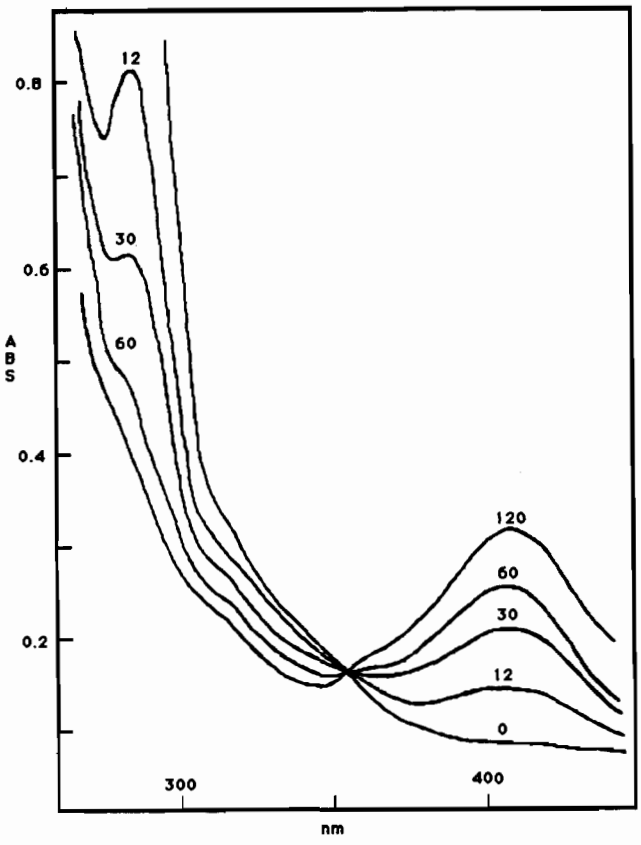


**Figure 1.** Spectral changes during 350-nm photolysis of $2.57 \times 10^{-7}$ mol of $W(CO)_6$(ads)/g of PVG in vacuo. Numbers designate photolysis times in seconds.

which appear as low-intensity shoulders on the above charge-transfer transitions in solution spectra,[33] appear as an unresolved tail in the 300–350-nm region. The molar extinction coefficients of the adsorbed complexes, calculated by assuming an optical path length equivalent to the penetration depth, are 15–20% larger than those in *n*-hexane solution. The actual difference is most likely smaller since there is an inherent spectroscopic uncertainty of ≤8% from sample to sample and a 20% uncertainty in penetration depth.[29] The latter describes cross-sectional distribution in the general sense but is not an accurate measure of the optical path length. DRIFT spectra of $Cr(CO)_6$(ads), $Mo(CO)_6$(ads), and $W(CO)_6$(ads) show intense bands centered at 1999, 2005, and 1986 $cm^{-1}$, respectively. With the exception of some broadening, particularly the lower energy shoulders, these spectra also resemble the spectra of the complexes in *n*-hexane.[11]

**Photochemical Reactions of $Cr(CO)_6$(ads), $Mo(CO)_6$(ads), and $W(CO)_6$(ads).** Excitation with 350-nm light causes an immediate decline in the UV absorption characteristic of each hexacarbonyl and a concurrent growth of bands in the 240–250- and 400–450-nm regions. Figure 1, which is representative of each complex, illustrates the spectral changes during a 350-nm photolysis of $2.57 \times 10^{-7}$ mol of $W(CO)_6$(ads)/g of PVG in vacuo. Maintainance of the isosbestic points and the reversibility of the reaction, however, vary from complex to complex. The bright yellow of $Cr(CO)_5$(ads), due to an absorption at 448 nm, fades considerably in the time required to transfer the cell to the spectrophotometer, whereas the intensity of the 410-nm absorption of $W(CO)_5$ declines ≤4%, after photolysis. With $W(CO)_6$(ads), the isosbestic point at 358 nm (Figure 1) is maintained through 40% reaction. With $Cr(CO)_6$(ads), the isosbestic point occurs at 360 nm and is maintained through ≤15% reaction, while that for $Mo(CO)_6$(ads) exists only for the first few percent of reaction. With each complex, the initial spectral changes are independent of surface coverage, and if the isosbestic point is maintained, GC analysis of the cell contents after 350-nm photolysis in vacuo yields 1.0 ± 0.1 mol of CO/mol of $M(CO)_6$ reacted; the latter is determined from the decrease in UV absorbance of the hexacarbonyl. The

**Table I.** Quantum Yields for Decarbonylation during 350-nm Photolysis and Estimates of the Quantum Yields of $CH_4$ Evolution during 310- and 254-nm Photolyses

| complex | $\phi^{a,b}$ | $\phi_M{}^b$ 310 nm | $\phi_M{}^b$ 254 nm |
|---|---|---|---|
| $Cr(CO)_6$ | 0.081 ± 0.025 | 0.03 | 0.002 |
| $Mo(CO)_6$ | 0.79 ± 0.10 | 0.10 | 0.008 |
| $W(CO)_6$ | 0.84 ± 0.09 | 0.14 | 0.01 |

[a] Quantum yield for reaction 1. [b] Estimated uncertainty of ±25% (see Experimental Section).

reaction stoichiometry and the similarity of the photoproduct spectra with those of the corresponding pentacarbonyls generated in low-temperature matrices[34,35] establish the primary photochemical event to be

$$M(CO)_6(ads) \rightarrow M(CO)_5(ads) + CO \qquad (1)$$

Perutz and Turner attribute the changes in band maxima of the individual pentacarbonyls generated in low-temperature matrices to an occupation of the vacated coordination site by the different matrix atoms or molecules.[34] The band maxima of the photoproducts on PVG resemble those of $M(CO)_5L$ complexes, where L denotes an O-donor ligand. For example, the band maximum of $W(CO)_5$(ads) occurs at 410 nm, while those of $W(CO)_5(Me_2CO)$ and $W(CO)_5(Et_2CO)$ occur at 406 and 418 nm, respectively.[25] Since the surface functionalities of a hydroxylated support are potential nucleophiles, $M(CO)_5$(ads) denotes a pentacarbonyl with the vacated coordination site occupied by an oxygen atom from either a silanol group or chemisorbed water. The absence of EPR resonances after 15–35% conversion to the photoproducts suggests that $M(CO)_5$(ads) has a $C_{4v}$ structure.[11] If the isosbestic point is maintained during photolysis, reaction 1 is reversible, and exposure to CO (1 atm) regenerates the hexacarbonyl in ≥96% yield.

In the presence of $O_2$ (1 atm), photolysis of the adsorbed complexes leads to irreversible oxidation. A rapid evolution of 5.9 ± 0.2 mol of CO/mol of adsorbed complex occurs during photolysis, and there is no spectrally detectable reversibility on exposure to CO (1 atm).

The isosbestic points observed during 350-nm photolyses are not present during 310- and 254-nm photolyses. However, the initial spectral changes, which consist of the immediate growth of bands in the 240–250- and 400–450-nm regions, indicate that the primary photochemical reaction of each adsorbed complex, i.e., reaction 1, is independent of excitation wavelength. Accurate quantum yield measurements are restricted to 350-nm excitation, where absorption by PVG is negligible. The values for reaction 1, extrapolated from plots of $\phi_{obsd}$ (corrected for thermal reversibility by extrapolating the spectral change back to the end of photolysis) vs irradiation time, are summarized in Table I.

The primary photochemical reaction is independent of the excitation wavelength, whereas the secondary photochemistry exhibits a marked dependence on excitation wavelength. Although the following focuses on $W(CO)_6$(ads), since most experiments were performed with this complex, the reactivities of the Mo and Cr analogues are essentially equivalent. Continued 350-nm photolysis of $M(CO)_5$(ads) causes further CO evolution. With $W(CO)_6$(ads), the yield of CO approaches the limiting value 1.1 ± 0.2 mol of CO/mol of hexacarbonyl adsorbed. The stoichiometry suggests a straightforward formation of the pentacarbonyl; however, electronic spectra indicate a more complex reaction sequence. A loss of the isosbestic point at 358 nm is accompanied by a decline and nondescript broadening of the photoproduct absorption at 410 nm. With samples containing $\geq 10^{-5}$ mol of $M(CO)_6$(ads), there is no spectral indication in the 475–550-nm region of the formation of dimeric or higher order cluster compounds.[36,37] Most likely, the stoichiometric mea-

(34) Perutz, R. N.; Turner, J. J. *J. Am. Chem. Soc.* **1975**, *97*, 4791–4800.
(35) Graham, M. A.; Poliakoff, M.; Turner, J. J. *J. Chem. Soc. A* **1971**, 2939–2948.

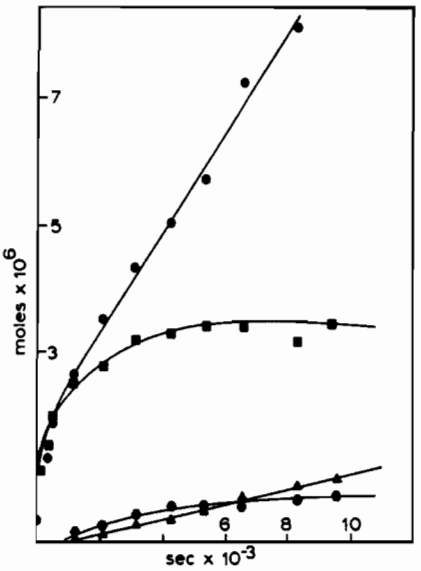


**Figure 2.** Yields of CO (●), $CH_4$ (▲), $H_2$ (●), and $W(CO)_5$(ads) (■) during 310-nm photolysis of $8.50 \times 10^{-6}$ mol of $W(CO)_6$/g of PVG.

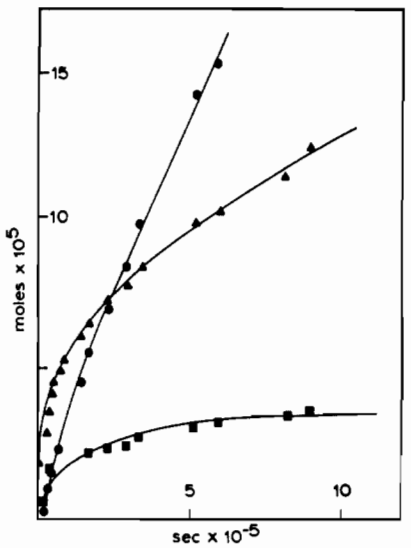


**Figure 3.** Yields of CO (▲), $CH_4$ (●), and $H_2$ (■) during 254-nm photolysis of $2.35 \times 10^{-5}$ mol of $W(CO)_6$/g of PVG.

surements are fortuitous, and the spectral broadening, although not resolved, corresponds to a composite spectrum of different monomeric $M(CO)_n$ ($n \leq 5$) species.[34] Nevertheless, the photochemistry with 350-nm excitation is limited to CO evolution.

**Methane Evolution.** Photolysis with 310- or 254-nm light leads to different reaction products. A 310-nm photolysis of a sample containing $8.50 \times 10^{-6}$ mol of $W(CO)_6$(ads)/g of PVG in vacuo (Figure 2) causes CO, $H_2$, and $CH_4$ evolution. Similar results occur with 254-nm excitation (Figure 3) except that the initial spectral changes indicative of $M(CO)_5$(ads) formation are not as well resolved. With both excitation wavelengths, $CO_2$ is also detected, but in trace amounts corresponding to ≤10% of the amount of $CH_4$ evolved. As described above, $CH_4$ evolution cannot be attributed to a decomposition of trace amounts of solvent, *n*-hexane, remaining in the glass. Furthermore, photolysis of samples prepared by solventless techniques, i.e., by sublimation of the complexes onto freshly calcined PVG samples, leads to $CH_4$ evolution within experimental error of that shown in Figure 2. Nor can $CH_4$ evolution be attributed to direct excitation of PVG (50% T at 295 nm vs air). PVG absorbs weakly at 310 nm and, particularly with less than monolayer coverage, is the dominant absorbing species at 254 nm. However, 310- or 254-nm photolysis of blank PVG under vacuum, under 0.1 atm of CO or $H_2$, or under a mixture of 0.1 atm of CO and 0.2 atm of $H_2$ does not result in $CH_4$ evolution.

Competitive absorption of the 310- and 254-nm excitation by the glass precludes an exact determination of the quantum yield of $CH_4$ evolution. To give some indication of the relative extent of this reaction pathway, however, estimates of the quantum yields of $CH_4$ evolution, $\phi_M$, computed from the initial rates of $CH_4$ evolution and the excitation intensity incident on the impregnated sample are listed in Table I. The lower values with 254-nm excitation, where a larger fraction of the excitation light is absorbed by the glass, are consistent with the observation that direct excitation of the unimpregnated glass does not lead to $CH_4$ evolution. The complex is essential to $CH_4$ evolution, and the $CH_4$ does not derive from *n*-hexane.

The absence of $CH_4$ evolution during the initial photochemical reaction (Figure 2) precludes the primary photoproduct species as the active reagent. During 254-nm photolysis, the isosbestic points are not present and the spectral changes indicative of $M(CO)_5$(ads) formation are not as well resolved. However, extrapolations of the initial rates of methane evolution (Figure 3) reveal a short induction period preceding $H_2$ and $CH_4$ evolution. CO evolution continues during the initial stages of the reaction, but eventually $CH_4$ becomes the dominant gaseous photoproduct. The rates of $CH_4$, $H_2$, and $CO_2$ evolution vary even within samples containing the same amount of complex, but the order of appearance of the gaseous photoproducts (Figures 2 and 3) is consistent from sample to sample and independent of the initial amount of adsorbed hexacarbonyl.

A 310- or 254-nm photolysis of the complexes adsorbed onto deuteriated PVG leads to the evolution of deuteriated methanes. Mass spectral analyses of the surrounding gas phase after 310-nm photolyses of deuteriated PVG samples containing $(5.2 \pm 0.1) \times 10^{-6}$ mol of $W(CO)_6$ reveal $CH_4$, $CH_3D$, and small amounts of $CH_2D_2$. The amount of deuteriated products increases with the extent of deuteriation of the glass (33–50%) but never exceeds 25% of the amount of $CH_4$ evolved. Thermal gravimetric analyses show that water is tenaciously held on PVG,[29] and a weak, high-frequency shoulder on the 2760-$cm^{-1}$ band of Si–OD indicates the presence of small amounts of chemisorbed $D_2O$. Since a rapid exchange between the various hydroxyl moieties is expected, these data only designate the silanol group and/or chemisorbed water as the hydrogen source.

$CH_4$ evolution is independent of surface coverage and occurs from samples containing from $10^{-7}$ to $10^{-3}$ mol of $W(CO)_6$(ads), which correspond to surface coverages ranging from 0.0008 to essentially monolayer coverage within the impregnated volumes. Nor is there spectral evidence of dimer formation or an intermediate metal hydride. A 310-nm photolysis of a sample containing $9.26 \times 10^{-6}$ mol of $W(CO)_6$(ads) causes the evolution of $7.54 \times 10^{-6}$ mol of $CH_4$. Assuming that the spectrum of a dimeric species on the glass resembles that of $[W_2(\eta^5\text{-}C_5H_5)_2(CO)_6]$, which exhibits bands at 362 nm ($\epsilon = 2.02 \times 10^4$ $M^{-1}$ $cm^{-1}$) and 493 nm ($\epsilon = 2.45 \times 10^3$ $M^{-1}$ $cm^{-1}$),[36] the spectral changes at 358 nm, the initial isosbestic point (Figure 1), and at 493 nm indicate that $\leq 10^{-8}$ mol of dimer is formed. Similarly, there is no spectroscopic indication of the formation of dimeric complexes during photolysis of the Cr and Mo analogues.[37] In fluid solution, $[(C_2H_5)_4N][HW(CO)_5]$ exhibits a band at 450 nm ($\epsilon = 4.6 \times 10^4$ $M^{-1}$ $cm^{-1}$) and a similar band when adsorbed onto PVG. During $CH_4$ evolution, the 410-nm band of $W(CO)_5$ declines and shows a nondescript broadening. A distinct band at 450 nm does not appear, and the optical density changes at 450 nm indicate that $\leq 10^{-9}$ mol of hydride is present. Furthermore, 254-nm photolysis of a PVG sample containing $1.3 \times 10^{-6}$ mol of $[(C_2H_5)_4N][HW(CO)_5]$/g of PVG in vacuo does not result in either a spectral change or the evolution of gaseous photoproducts.

Initially, $H_2$ evolution accompanies $CH_4$ evolution (Figures 2 and 3). $H_2$ evolution suggests metal oxidation, and EPR confirms its occurrence. EPR spectra recorded during 254-nm photolysis of crushed (60–80 mesh) PVG containing $7.83 \times 10^{-6}$ mol of

(36) Wrighton, M. S.; Ginley, D. S. *J. Am. Chem. Soc.* **1975**, *97*, 4246.
(37) Ginley, D. S.; Bock, C. R.; Wrighton, M. S. *Inorg. Chim. Acta* **1977**, *23*, 85.

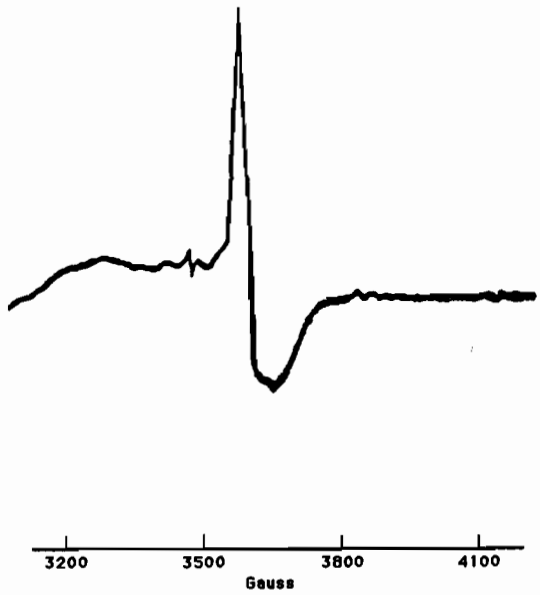


**Figure 4.** EPR spectrum generated during 254-nm photolysis of 7.83 × $10^{-6}$ mol of $Mo(CO)_6$(ads)/g of crushed (60–80 mesh) PVG.

$Mo(CO)_6$ in vacuo results in the appearance (Figure 4) of a resonance with $g = 1.948 \pm 0.002$ and peak width of 75 G. No resonance occurs when blank, calcined PVG (60–80 mesh) is irradiated under identical conditions. The signal intensity increases with increasing irradiation time, and GC analysis of the surrounding gas phase confirms the presence of $CH_4$. The EPR resonance is in excellent agreement with that described by Howe and Leith and establishes the formation of the Mo(V) hydrous oxide, $MoO_2(OH)$.[38] EPR resonances are not detected during similar experiments with $Cr(CO)_6$(ads) and $W(CO)_6$(ads). After extensive 310- or 254-nm photolysis of the latter, however, there is no reversibility when it is exposed to CO and electronic spectra are consistent with metal oxidation. The $W(CO)_6$(ads) samples become light blue and the electronic spectra, having a sharp spectral cutoff with 50% T at 465 nm, are essentially identical with spectra of $WO_3$ powder dispersed on the glass.

**Stoichiometric Measurements.** Since the oxidized metal will not react with CO, the stoichiometry of the oxidation accompanying $CH_4$ formation was determined by recovering the unoxidized metal as the hexacarbonyl. The number of moles of $CH_4$ evolved was determined by gas chromatography while the moles of hexacarbonyl consumed during photolysis of a sample containing 4.02 × $10^{-6}$ mol of $W(CO)_6$/g of PVG, $n_c$, was determined from the decline in the UV absorbance of the complex. The sample was then exposed to CO (1 atm), and the moles of hexacarbonyl regenerated, $n_r$, was calculated from the spectral change at 280 nm. A plot of the moles of complex irreversibly oxidized, $n_c - n_r$, vs the moles of $CH_4$ evolved (Figure 5) shows that oxidation of the metal initially occurs in a 1:1 stoichiometric ratio with the moles of $CH_4$ evolved. At the onset of $CH_4$ evolution during 310-nm photolysis of a sample containing 9.77 × $10^{-6}$ mol of $W(CO)_6$(ads), a total of 1.73 × $10^{-5}$ mol of CO has been evolved. This corresponds to an average loss of 1.8 mol of CO/mol of complex reacted. A series of measurements with samples containing from 5 × $10^{-6}$ to 5 × $10^{-5}$ mol of $W(CO)_6$ yield an average adsorbate stoichiometry at the onset of $CH_4$ evolution of $W(CO)_{4.0\pm0.2}$.

**Diffuse-Reflectance FTIR.** DRIFT spectra recorded during 254-nm photolyses of PVG (325 mesh) containing 2.06 × $10^{-5}$ mol of $W(CO)_6$(ads) (Figure 6a) show that the growth of weak bands at 1965 and 1932 $cm^{-1}$ accompanies the decline in the intensity of the 1988-$cm^{-1}$ band of hexacarbonyl. The 1965- and 1932-$cm^{-1}$ bands agree with the intense 1967- and 1926-$cm^{-1}$ bands of $W(CO)_5$ generated in a 20 K $CH_4$ matrix[34] and are

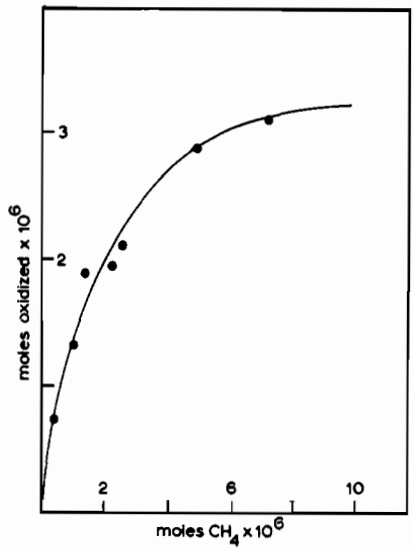


**Figure 5.** Moles of $W(CO)_6$ irreversibly oxidized, $n_c - n_r$ (see text), vs the moles of $CH_4$ evolved.

assigned to surface-bound pentacarbonyl. Consistent with electronic spectra, which indicate efficient secondary photolysis, the intensities of the 1965- and 1932-$cm^{-1}$ bands of the pentacarbonyl increase only during the first 15 s of photolysis. Continued photolysis causes these bands to decline with the accompanying appearance of weak bands at 1949 and 1894 $cm^{-1}$. Although weak, these features appear in each experiment and are in reasonable agreement with the prominent 1945- and 1887-$cm^{-1}$ bands of $W(CO)_4$.[28] The bands assigned to the tetracarbonyl do not increase on continued photolysis. Instead, the entire $\nu_{CO}$ region degrades without the appearance of lower wavenumber bands assignable to $W(CO)_n$ ($n \leq 3$) species.[34]

The decline in band intensity in the CO region, which eventually becomes transparent, is accompanied by the appearance of bands (Figure 6b) in the initially transparent C–H region. After 15 s, difference spectra reveal an absorption centered at 2964 $cm^{-1}$. The band intensity increases during photolysis and, after 45 s, resolves into peaks at 2967 and 2961 $cm^{-1}$. A distinct shoulder is also apparent at 2940 $cm^{-1}$ as well as a broad absorption in the 3210–3450-$cm^{-1}$ region. Other than changes in band shape, i.e., the 2967- and 2961-$cm^{-1}$ bands often appeared as a broader absorption centered at 2965 $cm^{-1}$, no further change in band intensity occurs during an additional 30-min photolysis. The strong absorptions due to PVG preclude detection of bands at ≤1900 $cm^{-1}$. In the high-wavelength region, however, the photoproduct spectrum agrees with the spectrum of formaldehyde adsorbed onto PVG, which exhibits a strong absorption at 2966 $cm^{-1}$ with a shoulder at 2945 $cm^{-1}$ and a broad absorption in the 3210–3450-$cm^{-1}$ region.

**Isotope Labeling.** Since the surface of PVG closely resembles that of silica gel[22-24] and the gaseous photoproducts in these experiments as well as their order of appearance parallel those found in the temperature-programmed decomposition of these hexacarbonyls on silica gel,[39,40] we initially assumed that $CH_4$ derived from coordinated CO with an accompanying oxidation of the metal atom. However, $CH_4$ evolution becomes independent of metal oxidation (Figure 5). In fact, GC analysis after exhaustive 254-nm photolysis of a sample containing 2.30 × $10^{-5}$ mol of $W(CO)_6$ reveals, in addition to 2.52 × $10^{-4}$ mol of $CH_4$, 1.35 × $10^{-4}$ mol of CO, which corresponds to a recovery of 98% of the CO initially coordinated to the metal. A series of experiments with samples containing from 6.31 × $10^{-6}$ to 4.33 × $10^{-5}$ mol of $W(CO)_6$(ads)/g of PVG confirmed that the amount of CO recovered corresponded to 94–98% of the CO originally coordinated to the metal. This raises a question regarding the source

(38) Howe, R. F.; Leith, I. R. *J. Chem. Soc., Faraday Trans.* **1973**, *69*, 1967–1977.

(39) Brenner, A.; Hucul, D. A.; Hardwick, S. J. *Inorg. Chem.* **1979**, *18*, 1478–1484.

(40) Brenner, A.; Hucul, D. A. *J. Am. Chem. Soc.* **1980**, *102*, 2484–2487.


**Figure 6.** DRIFT spectra during 254-nm photolysis of $2.06 \times 10^{-5}$ mol of $W(CO)_6$(ads)/g of powdered (320 mesh) PVG. Numbers in parentheses indicate photolysis times in seconds.

of $CH_4$, and $^{13}C$ labeling confirms that $CH_4$ does *not* derive from the coordinated CO. After 310-nm photolyses of PVG samples containing $3.62 \times 10^{-5}$ mol of $W(^{13}CO)_6$ (90% enriched), mass spectral analysis shows that ≤1% of the $^{13}C$ label appears in the evolved $CH_4$. Rather, 96 ± 1% of the label appears as evolved $^{13}CO$, which occurs in the expected 9:1 ratio, with the remaining 4 ± 1% appearing as evolved $CO_2$. Nineteen experiments with separate samples containing from $7.51 \times 10^{-6}$ to $5.30 \times 10^{-5}$ mol of labeled $W(^{13}CO)_6$ excited with either 254- or 310-nm light established that in all cases ≤1% of the label occurs in the evolved $CH_4$. The result is independent of whether the samples were initially prepared by solution impregnation or sublimation, i.e., solventless techniques. Clearly, the evolution of $CH_4$ derives from an impurity, yet it is *not* one that can be attributed to conventional impurity sources, such as residual amounts of the impregnating solvent, *n*-hexane, or adsorption of trace oils in the vacuum lines during sample manipulations. In the first place, $CH_4$ evolution occurs from freshly calcined samples impregnated by solventless techniques. Furthermore, both impurity sources would be expected to show, in addition to gaseous photoproducts, either the fragmentation pattern characteristic of *n*-hexane or peaks in the higher *m/e* range arising from the decomposition of an adsorbed oil. Yet neither is detected. To further test the possibility of contamination, a freshly calcined sample at ca. 500 °C was transferred to a photolysis cell with a side arm containing $W(CO)_6$. The portion of the cell containing the glass sample was placed in a sand bath at 250 °C, and the entire apparatus, including the solid complex at room temperature (22 ± 1 °C), was evacuated to $p \leq 10^{-4}$ Torr. The cell was then closed off, and after the system was cooled to room temperature, the complex was sublimed onto the glass sample. Again, mass spectra of the gas phase after 254-nm photolysis showed the presence of only CO, $H_2$, $CH_4$, and $CO_2$.

In all experiments, including those with the labeled complex, mass spectra of the surrounding gas show that unlabeled $CH_4$ is the sole hydrocarbon detected, and the highest *m/e* peak in the spectra occurs at 45, which corresponds to $^{13}CO_2$. Since $CH_4$ evolution occurs from samples that had been calcined at 650 °C for at least 72 h, and in some cases as long as 1 week, $CH_4$ does not derive from an adsorbed hydrocarbon. Rather, since the C source withstands the calcination conditions, we believe that $CH_4$ evolution arises from a metal-promoted reduction of a $C_1$ oxide present in the glass matrix.[41-43] Burnham reports that the principal form of C in silica melts is $CO_3^{2-}$, which derives from the reaction of $CO_2$ with dangling $O_2^-$ functions of the melt.[43] Although analysis of the calcined PVG with an Hitachi SEM equipped with a PGT energy dispersive X-ray analysis accessory failed to resolve that attributable to the impurity from residual background carbon, elemental analysis of calcined PVG indicates trace amounts, ≤1%, of C that is thought to be a $C_1$ oxide in the glass matrix.[44] Prolonged photolysis over a period of days shows that the amount of $CH_4$ evolved falls within this impurity level, and upon consumption of the C impurity further gas evolution ceases. For example, prolonged 254-nm photolysis of a PVG sample containing $2.30 \times 10^{-5}$ mol of $W(CO)_6$ in vacuo leads to the evolution of $1.35 \times 10^{-4}$ mol of CO, which corresponds to recovery of 98% of the originally coordinated CO. $CH_4$ evolution increases during the initial stages of photolysis, achieves a steady-state rate, and then declines and ceases with no further gas evolution. The complex penetrates 0.5 ± 0.1 mm into the glass, which corresponds to an impregnation of 20% of the PVG sample. Assuming that the C impurity converted to $CH_4$ is that within these initially impregnated volumes, the total moles of $CH_4$ evolved in the experiment, $2.52 \times 10^{-4}$ mol, corresponds to a C impurity level, 0.34 ± 0.07%, that lies within the reported impurity levels.[44]

## Discussion

In fluid solution, UV photolysis of the group 6B hexacarbonyls results in CO dissociation and in the presence of a nucleophile, L, formation of $M(CO)_5L$. Studies in low-temperature matrices confirm the formation of the corresponding pentacarbonyls[34,35] and support a reaction sequence where the primary photochemical step is CO dissociation followed by rapid scavenging of the pen-

(41) Reference 22, p 3.
(42) (a) Dake, H. C.; Fleener, F. L.; Wilson, B. H. *Quartz Family Minerals*; McGraw-Hill: New York, 1938. (b) Cameron, E. N.; Row, R. B.; Weis, P. L. *Am. Mineral.* **1953**, *38*, 218–262. (c) Roedder, E. *Rev. Mineral.* **1984**, *12*, 525.
(43) Burnham, C. W. In *The Evolution of the Igneous Rocks*; Yoder, H. S., Ed.; Princeton University Press: Princeton, NJ; 1979; p 454.
(44) Morse, D. L., private communication, Corning Glass Works, 1984.

tacarbonyl by an available nucleophile. Strohmeier and co-workers report initial quantum yields for $M(CO)_5L$ formation, ca. 1, that indicate a primary photochemical event of high efficiency.[45] On the other hand, Nasielski and Cola report a limiting quantum yield for the photosubstitution of CO by pyridine in $Cr(CO)_6$ of 0.67 ± 0.2.[46] In spite of the uncertainty, it is agreed that a relatively efficient loss of CO from these complexes is followed by rapid nucleophilic addition to the pentacarbonyl.[48]

DRIFT spectra of calcined PVG indicate a surface composed of free and associated silanol groups as well as small amounts of chemisorbed water. Chemically, the surface resembles that of silica gel except that Lewis acid sites, principally $B_2O_3$, are also present.[22-24] However, spectral data do not indicate any preferential adsorption of these or other complexes onto these sites.[12,13,29] Adsorption, either from fluid solution or by sublimation, is a random process leading to a uniform distribution of the hexacarbonyls on the surface. As found with other metal complexes,[12,13,28,29,31] the hexacarbonyls penetrate 0.5 ± 0.1 mm into the glass, and the penetration depth is taken as a measure of the deviation from surface planarity rather than population of the interior cavities of the glass. Consequently, the photochemical reactions examined in these experiments are limited to molecules on the outer, albeit highly irregular,[47] surfaces of PVG.

The absence of decomposition products, such as CO or $H_2$, during adsorption as well as the similarity of spectra of the adsorbed complexes with fluid-solution spectra establish that the complexes physisorb onto PVG as distinct molecular entities without disruption or significant distortion of their primary coordination spheres.[11] Therefore, changes in photoreactivity relative to that found in fluid solution cannot be attributed to a molecular change in the adsorbed complex. In fact, the initial photoreactions of the adsorbed complexes, particularly those during 350-nm excitation, exactly parallel that found in fluid solution.[48] The evolution of 1.0 ± 0.1 mol of CO/mol of complex consumed, the similarity of the photoproduct spectra (Figure 1) with spectra of the corresponding pentacarbonyls generated in low-temperature matrices,[34,35] and the recovery of ≥96% of the hexacarbonyl on exposure to CO (1 atm) establish reaction 1 as the primary photochemical event. Although isosbestic points are not observed during 310- and 254-nm photolysis (see below), the similarity of the initial spectral changes with those during 350-nm photolysis indicates that the primary photoreaction, i.e., reaction 1, is independent of excitation wavelength.

The absence of EPR resonances during 350-nm photolysis and the similarity of the photoproduct spectra with those of known $M(CO)_5$(O-donor) complexes are consistent with the singlet ground state of a square-pyramidal structure with the vacated coordination site occupied by an oxygen atom.[11] In spite of the relatively small amount of chemisorbed water on the calcined glass, recent studies of physisorbed $Fe(CO)_5$ indicate that the primary, tetracarbonyl, photoproduct reacts with either chemisorbed water or a silanol group, the latter being the more stable product.[12] Most likely, similar reaction pathways are accessible to the pentacarbonyls generated in these experiments. Both pentacarbonyl adducts would be expected to exhibit similar electronic spectra with bands in the 400–450-nm region. However, the short lifetime of the $Fe(CO)_4{\cdot}H_2O$ adduct, ≤100 s in vacuo,[12] suggests that the photoproduct spectra recorded in these experiments (Figure 1) are principally those of the silanol adduct. Consequently, $M(CO)_5$(ads) designates a $C_{4v}$ species where the silanol group binds the pentacarbonyl to the glass. Whether this represents a formal coordination to the glass, however, is not clear. Perutz and Turner report that the electronic spectra of the pentacarbonyls generated in Ar, $CH_4$, and $N_2$ matrices are sensitive to the matrix atom or molecule occupying the vacated coordination site.[34] Since the latter must be regarded as very weak ligands, the similarity with spectra of $W(CO)_5$(O-donor) complexes does not necessarily imply, in our opinion, a formal coordination to the glass. Furthermore, the activation energy, ≤7 kcal/mol,[49] for the thermal back-reaction

$$W(CO)_5(ads) + CO \rightarrow W(CO)_6 \qquad (2)$$

is considerably smaller than that for the substitution reactions of $W(CO)_5L$ complexes in fluid solution.[49] If overcoming the $W(CO)_5$–PVG interaction is the rate-determining step, then the activation energy suggests an interaction that, at least energetically, is significantly less than formal coordination to the silanol group. Of course, any attempt to draw thermodynamic conclusions from kinetic data is suspect. Nevertheless, the interaction with the glass stabilizes the primary, pentacarbonyl, photoproduct,[11] and as found in fluid solution, where the quantum yield of decomposition reflects a competition between addition of CO and an available nucleophile,[45] the quantum yields of decomposition of the adsorbed complex (Table I) reflect a competition between addition of CO and the silanol group.

Although dependent on previous heatings, studies of a variety of hydroxylated silicas indicate 4–7 silanol groups/100 Å$^2$.[51,52] If 3.5 Å is taken as the radius of $M(CO)_6$,[32] the planar surface area covered by the adsorbed carbonyl, 38.5 Å$^2$, places one to three silanol groups in the immediate vicinity of the photoproduct. Therefore, the quantum yields of formation of $M(CO)_5$(ads) (Table I) are not limited by the availability of silanol groups. In fact, the yields for $Mo(CO)_5$(ads), 0.79 ± 0.10, and $W(CO)_5$(ads), 0.84 ± 0.09, are comparable to the reported yields in fluid solution.[45,46] However, that for $Cr(CO)_5$(ads), 0.081 ± 0.02, is significantly smaller than the reported solution value, 0.67 ± 0.2.[46] This difference in yields is not due to a cage effect or a change in the adsorbate's photophysical properties. The electronic spectrum of $Cr(CO)_6$(ads), like that of the Mo and W analogues, is equivalent to that in fluid solution.[11] Since the cross-sectional distributions of each complex in the glass are identical within experimental error, a cage effect[53] that might arise from the low dimensionality of the PVG surface[47] would be independent of the metal complex, which is clearly not the case. Rather, the difference in yield must reflect a much weaker interaction between $Cr(CO)_5$(ads) and the silanol group. Unlike the case for $Mo(CO)_5$(ads) and $W(CO)_5$(ads), which show little reversibility, the significant decline in the 448-nm band of $Cr(CO)_5$(ads) and concurrent growth of the 280-nm band of $Cr(CO)_6$(ads) after photolysis indicate that the pentacarbonyl thermally reacts with the photodetached CO. A weaker interaction with the glass surface would facilitate a thermal reaction with the photodetached CO even after separation of the reaction pair and, in spite of the corrections for thermal reversibility, bias the subsequent calculation of the yield.

Reaction 1 is independent of excitation wavelength, whereas the secondary photochemistry is wavelength-dependent. With 350-nm excitation, CO evolution occurs, and in spite of a limiting stoichiometry of 1.1 ± 0.2 mol of CO/mol of $W(CO)_6$(ads) reacted, a loss of the isosbestic point and a decline and nondescript broadening of the initial $^1A \rightarrow {}^1E$ absorptions of the pentacarbonyl suggest the formation of $M(CO)_n$(ads) ($n \leq 5$) species.[34] The spectral change is independent of surface coverage and occurs without the appearance of lower energy bands attributable to polymeric species. The point to be emphasized, however, is that 350-nm excitation causes only CO evolution, whereas continued photolysis with 310- or 254-nm light leads to CO, $H_2$, $CH_4$, and $CO_2$ evolution (Figures 3 and 4).

The induction periods in Figures 2 and 3 establish that the pentacarbonyls are photochemically converted to a species that mediates $CH_4$ evolution. Stoichiometric measurements indicate that $CH_4$ evolution occurs when the complex achieves an average

(45) Strohmeier, W.; Gerlach, K. *Chem. Ber.* **1961**, *94*, 398–406.
(46) Nasielski, J.; Cola, A. *J. Organomet. Chem.* **1975**, *101*, 215–219.
(47) Evan, U.; Rademan, K.; Jortner, J.; Manor, M.; Reisfeld, R. *Phys. Rev. Lett.* **1984**, *52*, 2164–2167.
(48) Reference 33, p 69.
(49) Simon, R. C.; Morse, D. L.; Gafney, H. D. *Inorg. Chem.* **1985**, *24*, 2565–2570.
(50) Angelici, R. J. *Organomet. Chem. Rev., Sect. A* **1968**, *3*, 173–226.
(51) Snyder, L. R.; Ward, J. W. *J. Phys. Chem.* **1966**, *70*, 3941–3952.
(52) Reference 22, pp 622–714.
(53) Massey, A. G.; Orgel, L. E. *Nature (London)* **1961**, *191*, 1387.

molecularity of $W(CO)_4$. The molecularity is clearly an average, but it is consistent with the temperature-programmed decomposition of these complexes on silica gel[39,40] and the absence of lower frequency bands attributable to $W(CO)_n$ ($n \leq 3$) species[34] during $CH_4$ evolution. In the temperature-programmed decomposition of these complexes on silica gel, Brenner and co-workers report that 2 mol of CO/mol of complex is evolved prior to the evolution of $CH_4$.[39,40] Since DRIFT spectra of a number of $Fe(CO)_n$ ($n \leq 4$) species on PVG have been recorded,[12] we believe that the absence of lower frequency bands attributable to $W(CO)_n$ ($n \leq 3$)[34] is not due simply to their low steady-state concentrations. Rather, their absence as well as the constant low intensity of the tetracarbonyl bands, regardless of the length and intensity of the excitation, is consistent with an oxidation that limits the steady-state amount of $W(CO)_4$ formed and prevents the formation of $W(CO)_n$ ($n \leq 3$) species.

The sudden susceptibility to oxidation when the complex achieves the molecularity $M(CO)_4$(ads) is attributed to an inability of the photoproduct to complete its coordination shell. As pointed out above, one to three silanol groups are in the immediate vicinity of the photogenerated pentacarbonyl. Consequently, the pentacarbonyl readily completes its coordination shell by binding to a single silanol group and is relatively stable on PVG.[11] The tetracarbonyl, on the other hand, is unable to achieve the same stability. Assuming that there is an average of 5 silanol groups/100 Å$^2$ and that these are present at the corners and center of a 10 × 10 Å square, spanning any two of these groups requires M–O (O being the silanol oxygen) bond lengths of ≥5 Å, considerably larger than known bond lengths.[32] Of course, the assumptions that the silanol groups are uniformly distributed is suspect since DRIFT spectra of the glass indicate the presence of both free and associated silanol groups.[23,24] However, this does not change the fundamental argument that, at some point during the photoinduced decarbonylation, the decarbonylated fragment is unable to complete its coordination shell by binding to the surface silanol groups. At this point, which our data and those of Brenner and co-workers[39,40] indicate occurs at an average molecularity of $M(CO)_4$, the photoproduct becomes significantly more susceptible to oxidation and as a result switches to a photoinduced reaction pathway leading to $CH_4$ evolution.

The change in the stoichiometry of $CH_4$ evolution (Figure 5) indicates two reaction pathways. Initially, $CH_4$ evolution occurs with a stoichiometric oxidation of the complex, whereas at later times, the evolution of the hydrocarbon becomes independent of metal oxidation. Both reactions are photochemically driven, yet neither involves hydrogenation of coordinated CO. Gas chromatograms show a recovery corresponding to 96 ± 2% of the initially coordinated CO, and $^{13}C$ labeling establishes that, within an experimental error of ≤1%, *none* of the photochemically evolved methane derives from the initially coordinated CO. The evolution of $CH_4$ is an impurity effect, but not one that derives from the more conventional impurity sources. Methane evolution from samples prepared by solventless techniques precludes the impregnating solvent, *n*-hexane, as the carbon source. The absence of higher molecular weight fragments, $m/e \geq 46$, in the mass spectra precludes contaminants that might have been adsorbed during manipulations of the sample on a vacuum line. These would have to be oils or hydrocarbons of sufficiently high molecular weight to withstanding degassing at $p \leq 10^{-4}$ Torr and 250 °C. Since the total amount of $CH_4$ evolved falls within the known C impurity level in the glass, ≤1%,[44] the carbon source for $CH_4$ evolution is attributed to an impurity within the glass matrix. The nature of this impurity is not known,[41-43] but its ability to withstand the calcination conditions, in our opinion, precludes any type of hydrocarbon. A carbide would be thermally stable, but in view of the large amount of water initially present in PVG, we would expect that it would react with water and be desorbed as a hydrocarbon during calcination. Since $CH_4$ is the only hydrocarbon evolved, we believe that the impurity is a $C_1$ oxide within the glass matrix.[43] $CH_4$ derived from an impurity rather than coordinated CO would also account for the dependence of the $CH_4$ yield on the pretreatment of the glass. Extensive dehydration of the glass and calcination at 550 °C under flowing $H_2$ reduce the $CH_4$ yield during subsequent photolysis of the impregnated sample.

Consider first the stoichiometric conversion of the $C_1$ oxide to $CH_4$. As found in the temperature-programmed decomposition of $Cr(CO)_6$, $Mo(CO)_6$, and $W(CO)_6$ physisorbed onto silica gel,[39,40] the photoinduced evolution of $CH_4$ is also independent of the initial loadings, which in our experiments correspond to surface coverages ranging from 0.0008 to essentially monolayer coverage. In addition, there is no indication in either the electronic or DRIFT spectra of dimer, $\leq 10^{-8}$ mol, or higher order cluster formation.[36,37] Consequently, clusterification is not a prerequisite to photoinduced $CH_4$ evolution with these complexes. This is not the case with other complexes. A 254-nm photolysis of $Fe(CO)_5$ physisorbed onto PVG, for example, does not result in $CH_4$ evolution,[12] whereas photolysis of $Fe_3(CO)_{12}$ physisorbed onto PVG does result in $CH_4$ evolution and iron oxide formation.[54] At least in these photochemical reactions on PVG, where $CH_4$ derives from an impurity, whether clusterification is a necessary prerequisite appears to depend on whether the individual metal can supply an adequate number of reducing equivalents (see below).

EPR spectra (Figure 4) confirm the formation of $MoO_2OH$,[38] but an eventual decline in resonance intensity suggests that Mo(V) is an intermediate oxidation state. In the reduction of coordinated dinitrogen, Chatt and co-workers have shown that mononuclear complexes of Mo and W supply six reducing equivalents.[55] Optical spectra recorded after extensive photolyses indicate complete oxidation of the metal atom, i.e., formation of $WO_3$. Since the fully oxidized metal, having no unpaired electrons, would not be EPR-active, $CH_4$ evolution occurs with complete oxidation, where the individual metal atom supplies six reducing equivalents.

Concurrent with the oxidation is the appearance of bands (Figure 6b) in the initially transparent C–H region and a weaker, broad absorption in the 3210–3450-cm$^{-1}$ region. Rathke and Feder report the formation of methanol and methyl formate in the cobalt–carbonyl-catalyzed hydrogenation of CO.[56] Fahey reports the trapping of formaldehyde and glycolaldehyde intermediates in the homogeneous hydrogenation of CO and proposes that formaldehyde is the key intermediate in the reaction sequence.[57] Although strong absorptions of PVG preclude detection of lower frequency bands, the bands in the C–H and 3210–3450-cm$^{-1}$ regions agree with the bands of formaldehyde adsorbed onto PVG. In view of the above results and the fact that $CH_4$ is the sole hydrocarbon detected, the hydrogenation of the $C_1$ oxide proceeds through a formaldehyde and, although not detected in these experiments, most likely methanol intermediates. Unlike the hydrogenation of CO, i.e., the Fischer–Tropsch process,[58,59] where the CO is initially coordinated to the metal, however, the carbon source being hydrogenated in these photochemical experiments is not. Consequently, it is not clear whether these are coordinated intermediates. Of course, each could become coordinated, as has been suggested in the homogeneous reactions to compensate for the fact that the formation of formaldehyde from synthesis gas is thermodynamically unfavorable.[55] However, Fahey points out that the isolation of formaldehyde acetal argues that the formaldehyde need not be complexed even in homogeneous systems.[57] Furthermore, the spectral changes during the reaction (Figure 6) are not consistent with coordination. Roper and co-workers report that the formaldehyde complex $Os(\eta^2\text{-}CH_2O)(CO)_2(PPh_3)_2$ exhibits CO bands at 1977 and 1902 cm$^{-1}$.[61] As shown in Figure 6, however, the decline in the 1900–2000-cm$^{-1}$ $\nu_{CO}$ region during the time when there is a significant increase in the intensity in the C–H region argues against a coordinated formyl intermediate.

(54) Darsillo, M. S. Ph.D. Thesis, City University of New York, 1986.
(55) Chatt, J. *J. Organomet. Chem.* **1975**, *100*, 17–28.
(56) Rathke, J. W.; Feder, H. M. *J. Am. Chem. Soc.* **1978**, *100*, 3623–3625.
(57) Fahey, D. R. *J. Am. Chem. Soc.* **1981**, *103*, 136–141.
(58) Muetterties, E. L.; Stein, J. *Chem. Rev.* **1979**, *79*, 479–490.
(59) Masters, C. *Adv. Organomet. Chem.* **1979**, *17*, 61–100.
(60) Henrici-Olive, G.; Olive, S. *Angew. Chem., Int. Ed. Engl.* **1976**, *15*, 136–141.
(61) Brown, K. L.; Clark, G. R.; Headford, C. E. L.; Marsden, K.; Roper, W. R. *J. Am. Chem. Soc.* **1979**, *101*, 503–505.

Following reaction 1, which is independent of excitation wavelength, we propose that the following reaction sequence occurs with 310- or 254-nm excitation:

$$M(CO)_5(ads) \xrightarrow{h\nu} M(CO)_4(ads) + CO \quad (3)$$

$$M(CO)_4(ads) \xrightarrow{nh\nu} MO_3 + 4CO \quad (4)$$

$$H_2C{=}O \quad CH_3OH$$

$$C_1 \text{ oxide} \qquad CH_4$$

where $M(CO)_4$(ads), because of an inability to complete its coordination shell, undergoes a series of photoinduced oxidations. The wavelength dependence of reaction 4 indicates that oxidation of the tetracarbonyl requires ≥93 kcal/mol. Concurrent with the oxidation is the stoichiometric conversion of the $C_1$ oxide to formaldehyde, methanol, and ultimately $CH_4$. The reaction sequence is essentially equivalent to the Fischer–Tropsch hydrogenation[58] of CO except that the carbon being hydrogenated is not initially coordinated to the metal center. It is instead an impurity in the glass matrix, which we claim is a $C_1$ oxide.[43,44] There is no evidence in the analyses of PVG that this carbonaceous impurity agglomerates on the surface. Therefore, unlike the case for the Fischer–Tropsch process, where it is possible to increase the carbon chain length by successive additions of CO,[58] the carbon content of the product is limited by the carbon content of the impurity. Consequently, the hydrocarbon evolved in the above reaction sequence is, as experimentally found, limited to only $CH_4$.

Deuterium labeling designates the silanol group and/or chemisorbed water as the hydrogen source. The details of the transfer of hydrogen are not clear. There is no spectral evidence of an intermediate metal hydride, and 254-nm photolysis of $[(C_2H_5)_4N][HW(CO)_5]$ does not result in $CH_4$ evolution. However, we hesitate to rule out a hydride intermediate. The absence of a detectable absorbance at 450 nm may simply indicate a short-lived intermediate, whereas the lack of photoreactivity of the hydride may not be a fair comparison. Since the surface of PVG is anionic,[31] the hydride adsorbs as an associated salt. Consequently, its reactivity may not be equivalent to that of a hydride intermediate derived from a reaction of subcarbonyl with the glass surface.

Following the stoichiometric reaction, $CH_4$ evolution becomes independent of metal oxidation (Figure 5). Exhaustive 254-nm photolysis of a sample containing $2.30 \times 10^{-5}$ mol of $W(CO)_6$(ads), for example, evolves $2.52 \times 10^{-4}$ mol of $CH_4$ and $1.35 \times 10^{-4}$ mol of CO. Assuming that $2.30 \times 10^{-5}$ mol of $CH_4$ arises from the stoichiometric reaction, the majority of the $CH_4$, $2.29 \times 10^{-4}$ mol, evolves after oxidation of the metal atoms. During this stage of photolysis, the glass takes on a bluish tint and its electronic spectrum consists of a sharp cutoff (50% T at 465 nm) that closely resembles the spectrum of $WO_3$ powder dispersed on PVG. The appearance of a sharp spectral cutoff, as opposed to a spectrum composed of discrete transitions of individual molecular entities, is characteristic of an agglomerated metal oxide. Therefore, the metal oxide agglomerates during this stage of the reaction, and excitation of the agglomerate, which now possesses an electronic spectrum equivalent to that of a semiconducting solid,[62,63] catalyzes $CH_4$ evolution.

Photoinduced reductions on dispersed semiconductor particles, particularly $TiO_2$ particles, are well established.[62,63] Boonstra and Mutsaers report that UV photolysis of acetylene and ethylene in the presence of incompletely degassed powdered $TiO_2$ leads to the formation of $CH_4$, $C_2H_4$, $C_2H_6$, and $C_3$ hydrocarbons, whereas photolysis in the presence of completely outgassed $TiO_2$ yields benzene from $C_2H_2$ and 1-butene from $C_2H_4$.[64] The difference is attributed to the loss of chemisorbed water and a decline in the number of surface Ti–OH groups.[64] Schrauzer and others report the formation of $NH_3$ when powdered $TiO_2$ is irradiated in the presence of $N_2$.[65–68] In a recent paper, Endoh, Leland, and Bard describe a similar process on amorphous tungsten oxide films.[69] Excitation of blue amorphous oxide films, believed to be $WO_3$ and $WO_{2.96}$, in the presence of moist $N_2$ catalyzes the formation of $NH_3$.[69] Since the spectrum of the tungsten oxide generated on PVG closely resembles that described by Bard and co-workers,[69] we propose that the agglomerated oxide behaves as a semiconductor and, on excitation, facilitates the reduction of the carbonaceous impurity. Although their intensities are significantly lower during this stage of the reaction, the presence of the 2965- and 2977-$cm^{-1}$ bands assigned to formaldehyde suggests that reduction proceeds by the sequence of steps described for the stoichiometric reaction except that the metal no longer supplies the reducing equivalents. Rather, excitation of the metal oxide promotes the transfer of electrons to the $C_1$ impurity. The nature of the electron donor is not known, but in view of the previous results[64] and the dependence of $CH_4$ evolution on the extent of dehydration of the glass, we suspect that chemisorbed water is the ultimate electron source.

Not only is agglomeration essential to the formation of a semiconducting solid but its occurrence also indicates that the metal oxides and/or agglomerated oxides are mobile on the surface of the glass. Both events, i.e., formation of a solid with a spectrum like that of a semiconductor and the mobility of this species on the surface, are essential to the continued evolution of $CH_4$. Since the $CH_4$ evolved during this stage of the reaction continues to derive from the impurity distributed throughout the glass, mobility of the oxide and/or its agglomerate is essential to allow access of the metal oxide to the carbon source. In other words, the metal oxide photocatalyst randomly migrates to the carbon source rather than the more conventional migration of the carbon source to the catalyst. Consequently, the yield of methane is limited by the number of impurity sites and the mobility of the agglomerated metal oxide, which we expect to decline as the level of aggregation increases. Furthermore, in contrast to the concatenation of the hydrocarbons observed with $TiO_2$,[64] the carbon content of the evolved hydrocarbon is limited by the carbon content of the impurity and, hence, only $CH_4$ evolution occurs. Further work is in progress to elucidate the details of this proposed reaction scheme. Nevertheless, the evolution of $2.29 \times 10^{-4}$ mol of $CH_4$ after complete oxidation of the complex indicates that the agglomerated $WO_3$ is photocatalytic on the surface of PVG. Considering the parameters that control the photocatalytic evolution of $CH_4$ in these PVG samples, i.e., the number and distribution of the impurity sites and the mobility and level of aggregation of the metal oxide, it is not surprising that the turnover number, which for the above sample is 10:1, range from ca. 5:1 to a high of 12:1 in the samples examined.

## Conclusion

In spite of the similarity in both the initial gases evolved and their order of appearance with those observed during the thermal decomposition of these complexes on silica gel, GC analyses and $^{13}C$ labeling establishes that the photoinduced evolution of $CH_4$ derives *not* from the initially coordinated CO but from a carbonaceous impurity that we assign to a $C_1$ oxide in the glass matrix. Therefore, the composition of the impurity, rather than the nature of the complex, which acts simply as a source of electrons, controls the composition of the evolved hydrocarbon.

The photoinduced reduction of the impurity and the resulting evolution of $CH_4$ occurs by two reaction pathways. The first is a stoichiometric reduction in which the metal supplies six reducing

(62) Bard, A. J. *Science (Washington, D.C.)* **1980**, *207*, 139–144.
(63) Nozik, A. J. In *Photochemical Conversion and Storage of Solar Energy*; Connolly, J. S., Ed.; Academic: New York, 1981; pp 271–295.
(64) Boonstra, A. H.; Mutsaers, C. A. H. A. *J. Phys. Chem.* **1975**, *79*, 2025–2027.
(65) Schrauzer, G. N.; Guth, T. D. *J. Am. Chem. Soc.* **1977**, *99*, 7189–7193.
(66) Kahn, F.; Yue, P.; Rizzuti, L.; Augugliaro, V.; Schiavello, M. *J. Chem. Soc., Chem. Commun.* **1981**, 1049–1050.
(67) Li, Q.; Domen, K.; Naito, S.; Onishi, T.; Tamaru, K. *Chem. Lett.* **1983**, 321–324.
(68) Miyama, H.; Juji, N.; Nagae, Y. *Chem. Phys. Lett.* **1980**, *74*, 523–524.
(69) Endoh, E.; Leland, J. K.; Bard, A. J. *J. Phys. Chem.* **1986**, *90*, 6223–6226.

equivalents. After formation of the agglomerated metal oxide, the second is a photocatalyzed reduction of the impurity, where the agglomerated metal oxide behaves as a photoexcited semiconductor. Unlike thermal activation where $CH_4$ evolution is limited to a stoichiometric reaction,[39,40] optical excitation of the resulting agglomerated metal oxide continues to photocatalyze the evolution of $CH_4$. A significant question arising from these experiments is the nature of the carbonaceous impurity and, since the agglomerated metal oxide is a photocatalyst, whether this impurity can be replenished by reaction with a simple carbon oxide.

**Acknowledgment.** Support of this research by the Research Foundation of the City University of New York, Dow Chemical Co.'s Technology Acquisition Program, the National Science Foundation (Grant CHE-8511727), and the New York State Science & Technology Foundation (Grant SSF (85)-5) is gratefully acknowledged. H.D.G. thanks Queens College for a Presidential Research Fellowship during 1987, Professor W. F. Berkowitz for many helpful discussions, and the Corning Glass Works for samples of porous Vycor glass.

**Registry No.** $Cr(CO)_6$, 13007-92-6; $Mo(CO)_6$, 13939-06-5; $W(CO)_6$, 14040-11-0; $Cr(CO)_5$, 26319-33-5; $Mo(CO)_5$, 32312-17-7; $W(CO)_5$, 30395-19-8; $Cr(CO)_4$, 56110-59-9; $Mo(CO)_4$, 44780-98-5; $W(CO)_4$, 114221-02-2; CO, 630-08-0; $CH_4$, 74-82-8; $H_2$, 1333-74-0; $CO_2$, 124-38-9; formaldehyde, 50-00-0; methanol, 67-56-1.

---

Contribution from the Department of Inorganic Chemistry, University of Melbourne, Parkville, Victoria 3052, Australia

# Isolation and Crystal Structure of Manganese(II) Tetrafluoroborate: A Unique Example of Manganese(II) with Seven Unidentate Ligands

Russell W. Cockman, Bernard F. Hoskins,* Malcolm J. McCormick, and Thomas A. O'Donnell*

*Received January 5, 1988*

Crystalline manganese(II) tetrafluoroborate has been isolated as the ansolvate from a solution in anhydrous hydrogen fluoride. Its crystal structure provides the first instance of Mn(II) in a seven-coordinate environment of unidentate ligand atoms, each of which is derived as a terminal fluorine atom from a $BF_4$ group; the $MnF_7$ coordination polyhedron is a monocapped trigonal prism. There are two types of tetrahedral $BF_4$ groups, one bridging four manganese atoms through each of its fluorine atoms and the other bridging only three manganese atoms, giving the formula $Mn(BF_4)_{4/4}(BF_4)_{3/3}$. Crystals of $Mn(BF_4)_2$ are orthorhombic with the space group *Pnma*, $Z = 4$, and unit cell dimensions $a = 8.6042$ (9) Å, $b = 5.4496$ (4) Å, and $c = 10.8673$ (9) Å. The structure was refined by a full-matrix least-squares method from 491 statistically significant reflections.

## Introduction

Solubilities at room temperature of di- and trifluorides of d- and f-transition elements in "neutral" or natural anhydrous hydrogen fluoride (AHF) are very small, typically less than $5 \times 10^{-3}$ *m* for d-transition-metal difluorides and much less again for trifluorides. Consequently, until relatively recently, it was not possible to use spectroscopy to gain information about the solvation environment of cations in AHF or to crystallize transition-metal compounds from AHF for structural determination. Deliberate enhancement of the acidity of AHF by use of fluorides that are Lewis acids of the solvent system led to greatly increased concentrations of transition-metal cations in AHF[1,2] and has overcome the two experimental problems outlined above.

UV–visible spectra in AHF have been recorded for a very wide range of d- and f-transition-metal cations,[1,3-5] and these and ESR spectra[6] indicate that coordination numbers and stereochemistries of cations in AHF are very similar—usually identical—to those in water or in fluoride environments in solids. Specifically the coordination numbers in AHF are generally 6 for first-row elements,[1,5] 8–9 for the trivalent lanthanides,[7] at least 9 for the divalent ions $Sm^{2+}$, $Eu^{2+}$, and $Yb^{2+}$,[7] and 5 in the equatorial plane for $UO_2^{2+}$.[7] There is good evidence that coordination is by HF molecules, but the contribution made to the inner sphere by the counterions such as $SbF_6^-$, $AsF_6^-$, and $BF_4^-$ is not easily determined at the present time, though it is expected to be negligible especially in diluted solutions.[4,7]

An extension of the studies of solvation of cations in AHF has been the attemped isolation from AHF of crystalline salts containing HF-solvated cations. Within this context solutions of manganese(II) tetrafluoroborate, produced by treating $MnF_2$ with $BF_3$ in AHF, readily gave colorless, well-formed crystals on cooling or on evaporating solvent from saturated solutions. These crystals were the subject of an X-ray crystallographic investigation, the results of which are reported in this paper.

The solid has been characterized as $Mn(BF_4)_2$. From the general viewpoint of inorganic chemistry the unique feature of this structure is the monocapped-trigonal-prismatic coordination of the manganese center, the seven-coordination being achieved by fluorine atoms derived from well-defined "monodentate" tetrafluoroborate anions.

In an extensive review of seven-coordinate compounds in 1979 Kepert[8] commented on the very small number of compounds containing seven identical unidentate ligands and he listed six known examples, including the structurally simple $IF_7$. The only example from the first row of the d transition metals was $V(CN)_7^{4-}$. In several compounds seven-coordination has been virtually forced on manganese(II) by the use of multidentate ligands with simple ligands occupying a small number of sites. An early example was that of $H_2O$ bonded to the seventh site around Mn(II) when the other six were occupied by EDTA.[9] Other hexadentate ligands dictate similar stereochemistry.[10]

(1) Barraclough, C. G.; Cockman, R. W.; O'Donnell, T. A. *Inorg. Chem.* **1977**, *16*, 673.
(2) Court, T. L.; Dove, M. F. A. *J. Fluorine Chem.* **1975**, *6*, 491.
(3) Barraclough, C. G.; Cockman, R. W.; O'Donnell, T. A. *Inorg. Nucl. Chem. Lett.* **1981**, *17*, 83.
(4) Baluka, M.; Edelstein, N.; O'Donnell, T. A. *Inorg. Chem.* **1981**, *20*, 3279.
(5) Barraclough, C. G.; Cockman, R. W.; O'Donnell, T. A.; Schofield, W. S. J. *Inorg. Chem.* **1982**, *21*, 2519.
(6) Barraclough, C. G.; Cockman, R. W.; O'Donnell, T. A.; Snare, M. J., submitted for publication in *Inorg. Chem.*
(7) Cockman, R. W. Ph.D. Thesis, University of Melbourne, 1983.
(8) Kepert, D. L. In *Progress in Inorganic Chemistry*; Lippard, S. L., Ed.; Wiley: New York, 1979; Vol. 25, pp 41–144.
(9) Richards, S.; Pederson, B.; Silverton, J. V.; Hoard, J. L. *Inorg. Chem.* **1964**, *3*, 27.

0020-1669/88/1327-2742$01.50/0 